Multisensor Microwave Sea-Ice Classification

Quinn P. Remund, David G. Long, and Mark R. Drinkwater
Brigham Young University, MERS Laboratory
459 CB, Provo, UT 84602
801-378-4884, FAX: 801-378-6586
remundq@ee.byu.edu, long@ee.byu.edu, mrd@pacific.jpl.nasa.gov

Abstract— A knowledge of polar sea-ice extent, type, and location is a valuable tool in understanding many geophysical processes. This paper presents an iterative statistical technique for ice classification of multisensor remote sensing imagery. NSCAT, ERS-2, and SSM/I data are used to construct enhanced resolution images. Preprocessing consists of data standardization and principal component analysis dimensionality reduction. The iterative algorithm is developed based on maximum a posteriori (MAP) method with the assumption of a Gaussian conditional probability density of each ice type. The technique is applied to data collected during a six day imaging interval in September of 1996. For this application, the algorithm performs better than nearest neighbor, iterative maximum likelihood, or K-means approaches.

INTRODUCTION

Polar sea ice plays an important role in the global climate and several geophysical processes. Sea ice influences heat transfer between the ocean and atmosphere, regulates the amount of solar radiation reflected back into space, and is considered a sensitive indicator of long term climate change [1]. Consequently, a knowledge of sea ice characteristics is a valuable asset in understanding these important geophysical processes. These characteristics can be grouped into a number of different ice classes or types. Research in the field of microwave scatterometry and radiometry has shown correlations between sea ice parameters and observed microwave signatures. By combining these data sets in a classification algorithm, imagery depicting locations of different ice types can be generated. This paper describes the development and implementation of a multisensor iterative approach to sea ice classification of remote sensing imagery.

BACKGROUND

Data collected by three instruments, the NASA scatterometer (NSCAT), the AMI scatterometer aboard the European remote sensing satellite (ERS-2), and the Special Sensor Microwave/Imager (SSM/I) are used in the proposed classifier. NSCAT is a Ku-Band (14 GHz) dual-polarization scatterometer that flew from August of 1996 through June 1997. It measures σ^o, the normalized radar cross-section, at multiple incidence and azimuth angles. The AMI scatterometer aboard ERS-2 is similar to NSCAT in measurement collecting geometry operating at C-Band (5.3 GHz) and vertical polarization. SSM/I is a dual-polarization multi-frequency radiometer which measures brightness temperature T_B of the earth's surface. The SSM/I frequencies are approximately 19, 22, 37, and 85 GHz with v- and h-pol at all frequencies except 22 for which only v-pol measurements are taken. The several channels of each instrument are considered separate parameters to be used in the ice classification effort.

Enhanced resolution microwave imagery is created for each channel of the previously described instruments by combining data collected from multiple passes of each satellite during an imaging period. Since ERS-2 and NSCAT h-pol measurements require about 6 days for satisfactory coverage of the Antarctic ice cover, this period is used for the image reconstruction of all data parameters. The scatterometer image reconstruction (SIR) algorithm is used to generate the enhanced resolution images [2]. Since both NSCAT and ERS-2 collect σ^o measurements over a range of incidence angles, a linear model is used to characterize the observed responses over $\theta \in [20°, 55°]$

$$\sigma^\circ = A + B(\theta - 40°) \tag{1}$$

where A is σ^o at 40 degrees incidence and B is the incidence angle dependence of σ^o. A bivariate version of SIR generates A and B images for NSCAT v- and h-pol and ERS-2 v-pol. For SSM/I a univariate version of SIR is used to create T_B images for each channel [3]. This results in 13 possible parameters to be used in the classification "feature vector." Since the ERS-2 B images are relatively noisy, all parameters but this one are used in the algorithm.

In order to minimize the effects of ocean pixels on the distribution an ice masking algorithm is applied to all of the images. The method utilizes the NSCAT polarization response, incidence angle dependence, and azimuth/temporal dependence of σ^o to segment ocean from sea ice [4].

MULTIVARIATE ANALYSIS

The classification parameter data set consists of three different parameter types: A, B, and T_B. Since each has different units and ranges of values, standardization is required to ensure that some parameters are not given undue weight in the classification. In an effort to preserve the ice class dependent biases that may exist in each parameter

0-7803-5207-6/99/$10.00 © 1999 IEEE.

type, the following standardization technique is applied for a particular observation x

$$x_s = \frac{(x - \mu_{type})}{\sigma_{type}} \quad (2)$$

where μ_{type} and σ_{type} is the mean and standard deviation of all the data of a particular data type (e.g., all the SSM/I data) and x_s is the new standardized parameter value. Hence, all standardized A, B, and T_B data have zero mean and unit variance.

Principal component analysis (PCA) is then used to examine the variance structure and informational content of the 12-dimensional standardized data set. PCA achieves this through a linear transformation which rotates the data space. For standardized data, PCA uses an eigenvector/eigenvalue decomposition to construct the necessary orthonormal basis vectors. The eigenvalue/eigenvector equation is given by $K\Gamma = \Gamma\Lambda$ where K is the 12 x 12 covariance matrix of the standardized data, Γ is a matrix with eigenvectors of K along the columns (which form a basis for the original 12-dimensional space), and Λ is a diagonal matrix with the eigenvalues of K along the diagonal (which represent the variances spanned by each eigenvector). Once these are obtained, a 12 x 1 data vector $\vec{y}$ containing standardized parameters is transformed by $\vec{z} = \Gamma^T \vec{y}$. The top eigenvector spans the axis of maximum variance in the data. The next eigenvector points in the direction of highest variance in the data orthogonal to the top eigenvector and so on. Using this technique, principal component images are created. Each image represents a mixture of information contained in the original A, B, and T_B images. By observing the coefficients of the corresponding eigenvectors, the contribution of each original parameter to the principal component image can be assessed.

The PCA transformation orders the eigenvalues and eigenvectors by increasing variance values. For the imaging interval 1996 JD 261-266, much of the variance or informational content of the data is contained in the top few principal components. In this case, over 90% of the variance is spanned by the top three components while the lower components contain negligible information. In fact, the lower PCA images appear quite noisy and hence are not used in the classification, reducing computational complexity and memory requirements.

ITERATIVE ALGORITHM DEVELOPMENT

Several statistical methods hold potential for application in the classification problem. The proposed sea ice classification algorithm is a maximum a posteriori (MAP) technique maximizing the posterior distribution over all possible ice types

$$argmax_c\ p(C|\vec{z_t}) = argmax_c\ \frac{p(\vec{z_t}|C)p(C)}{p(\vec{z_t})} \quad (3)$$

where $\vec{z_t}$ is the principal component vector $\vec{z}$ truncated to the top three terms and C is a discrete variable denoting the ice type. Assuming that the conditional distributions $p(\vec{z_t}|C)$ are Gaussian, and after some mathematical manipulation, the maximization becomes

$$argmax_c\ [-\frac{1}{2}(log|K_c| + (\vec{z_t} - \vec{\mu}_c)^T K_c^{-1}(\vec{z_t} - \vec{\mu}_c)) \quad (4)$$
$$+log(p(C))]$$

where K_c and $\vec{\mu}_c$ are respectively the covariance matrix and mean vector of the data in principal component space for ice type c. While a rough idea of the centroid locations $\vec{\mu}_c$ can be obtained from limited training data, K_c and the *a priori* distribution $p(C)$ are generally unknown. However, estimates of these can be obtained in an iterative classification approach. The procedure uses the truncated principal component data and is defined as follows:

1. With an initial approximation for $p(C)$, perform a weighted nearest neighbor classification using $\vec{\mu}_c$ obtained from small training regions.
2. Compute estimates of K_c, $\vec{\mu}_c$, and $p(C)$.
3. Perform a MAP classification using these estimates and Eq. 4.
4. If converged, quit, otherwise go to step 2.

The algorithm iterates until it converges to a classification estimate. Simulations demonstrate that as long as the initial centroids are relatively near the real centroids, the algorithm converges to a solution that is close to the true MAP classification.

Termination of the iterative procedure is based on two convergence metrics. The first is the spectral norm of each of the covariance matrices K_c which is equivalent to the square root of the largest eigenvalue of $K_c^T K_c$ This provides a measure of the overall covariance structure of each of the ice type clusters. The second metric is simply the Euclidean norm of each of the cluster centroid vectors $\vec{\mu}_c$. Convergence of these measures indicates diminishing cluster deformation and centroid drift.

RESULTS

The algorithm is applied to A, B, and T_B imagery for the time interval 1996 JD 261-266. Training data for initial estimates of each $\vec{\mu}_c$ is obtained from regions selected on the basis of *in situ* field observations and existing radar image data. The chosen classes are grounded and drifting icebergs (IB), perennial ice (PER), rough first year ice (RFY), smooth first year ice (SFY), young ice (YNG), pancake ice (PNC), and the marginal ice zone (MIZ). Figure 1 shows plots of the matrix and centroid norms illustrating reasonable convergence after about 25 iterations of the algorithm. The resulting classified image is shown in Figure 2.

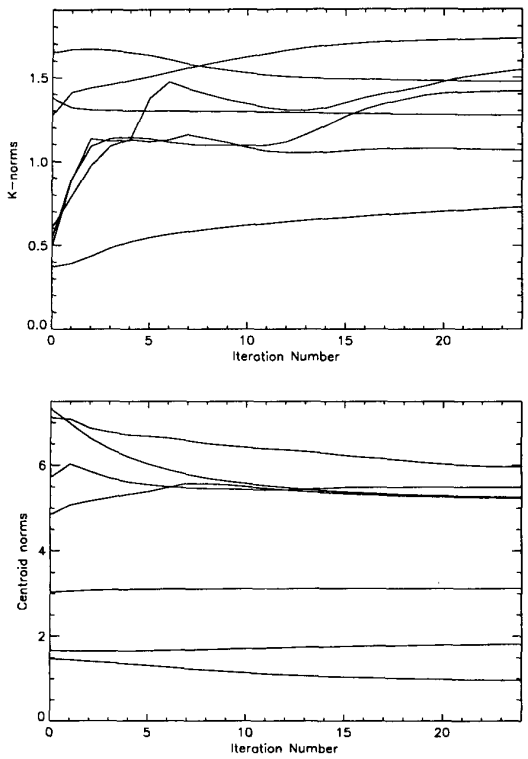

Figure 1: Covariance matrix norms (top) and centroid norms (top) demonstrating convergence of the algorithm.

High resolution SAR data provides an excellent means of validation for classification algorithms such as this. However, due to the inavailability of appreciable amounts of Antarctic SAR data during any given six day period, it is difficult to completely assess the accuracy of the resulting ice map. However, the general form of the ice locations is believable with respect to general ice dynamics (see Drinkwater paper in this conference). MIZ occurs in the outer margins of the ice pack. By day 266, only a small amount of perennial ice remains near the tip of the Antarctic Peninsula since much of the ice surviving the previous summer's melt is quickly swept northward by the Weddell Gyre and melted. Rough first year ice is found further out in the ice pack than smooth first year ice. This is consistent with the classification result obtained in [5] in which ERS-2 data trained with *in situ* data was used to determine ice type. On the other hand, there are some obvious classification errors. For instance, the large tongue extending from the Ross Ice Shelf is labeled RFY though this is a region of new ice production. This effect is likely caused by frost flower formation on young ice which emulates an RFY signature [6]. Also, a portion of the Ronne Ice Shelf which has advanced beyond the limit of the old ice shelf mask is misclassified as pancake ice by the algorithm. In the future, SAR data may be used to improve the choice of training regions as well

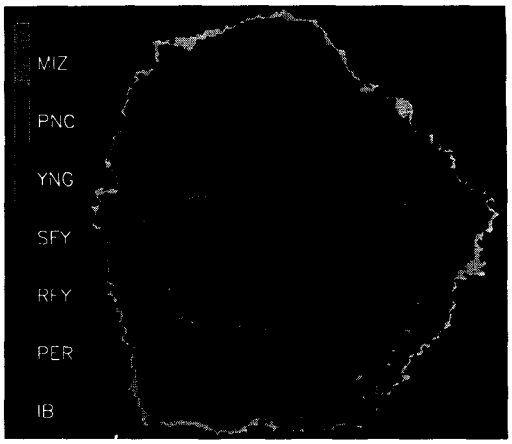

Figure 2: Classified image for 1996 JD 261-266.

as improve the classification. We are nonetheless limited to periods of sensor overlap.

When the algorithm is applied to a sequence of consecutive image sets, temporal stability in ice type classification is observed. While the lack of validation is a serious concern, this result indicates that the algorithm is certainly classifying features in the observed signatures. With proper training/validation data the algorithm is expected to produce even more satisfactory results.

This classification result was compared with three other classifications: nearest neighbor, iterative maximum likelihood, and K-means. While space prohibits showing the resulting classification images, it was found that the iterative MAP approach was superior to the others when using the same training regions. In particular, the other methods resulted in unreasonable classifications of the ice cover such as unrealistically large areas of icebergs and perennial ice.

REFERENCES

[1] W.F. Budd, "Antarctic sea ice variations from satellite sensing in relation to climate," *IEEE Trans. on Geosci. and Rem. Sens.*, vol. 15, pp. 417–426, 1975.

[2] D. Long, P. Hardin, and P. Whiting, "Resolution Enhancement of Spaceborne Scatterometer Data," *IEEE Trans. on Geosci. and Rem. Sens.*, vol. 31, pp. 700–715, 1993.

[3] D.G. Long and D.L. Daum, "Spatial Enhancement of SSM/I Data," *IEEE Trans. Geosci. Remote Sens.*, vol. 36, pp. 407–417, 1997.

[4] Q. Remund and D. Long, "Sea-Ice Extent Mapping Using Ku-Band Scatterometer Data," *in press J. Geophys. Res.*

[5] M. Drinkwater, "Satellite Microwave Radar Observations of Antarctic Sea Ice," in Analysis of SAR Data of the Polar Oceans, C. Tsatsoulis and R. Kwok, Eds. Berlin: Springer, 1998, pp. 145-188.

[6] M. Drinkwater and G. Crocker "Modelling changes in the dielectric and scattering properties of young snow-covered sea ice at GHz frequencies," *Journal of Glaciology,*, vol. 34, no. 118, pp. 274–282, 1988.